THE ASTROPHYSICAL JOURNAL, 467:145–161, 1996 August 10

CLASSICAL DOUBLE RADIO GALAXIES AND THEIR GASEOUS ENVIRONMENTS

LIN WAN AND RUTH A. DALY[1]
Department of Physics, Princeton University, Princeton, NJ 08544
Received 1995 August 9; accepted 1996 February 19

ABSTRACT

A sample of classical double radio galaxies has been constructed to study the effect of environment on radio sources. The sample consists of radio galaxies in cluster and noncluster environments and includes galaxies and clusters at both high ($z \sim 0.5$) and low ($z \sim 0$) redshift. Most of these radio galaxies are intermediate-power FR II sources with 408 MHz powers in the range from 10^{32} to 10^{35} h^{-2} ergs s^{-1} Hz^{-1}, where the upper bound corresponds roughly to a 178 MHz power of about 10^{27} h^{-2} W Hz^{-1} sr^{-1}. Comparisons are made between the properties of FR II radio galaxies in cluster and noncluster environments, and between X-ray clusters with and without FR II radio galaxies. The principal results are the following:

1. Most low-redshift FR II galaxies in clusters appear to be similar to FR II galaxies in group or field environments in terms of radio power, optical properties of the host galaxy, and nonthermal pressure of the radio bridge.
2. High-redshift FR II galaxies are all quite similar and do not appear to vary with galactic environment. The radio powers and emission-line luminosities of the host galaxies of high-redshift FR II sources are higher on average than their low-redshift counterparts, but there is also overlap, and the nonthermal pressures of the radio bridges appear to be independent of redshift.
3. The nonthermal pressures of the bridges of FR II sources appear to be similar to the thermal pressures of the ICM around them. This result, if confirmed by a larger sample, would allow the bridges of FR II sources to be used as probes of their gaseous environments.
4. The fact that most FR II galaxies have similar nonthermal pressures, irrespective of galactic environment and redshift, indicates that the gaseous environments around them are also similar. Typical nonthermal pressures of these FR II sources are much lower than typical thermal pressures of the ICM in X-ray bright clusters, suggesting that FR II sources are generally in environments with gas pressures much less than typical low-redshift ICM pressures.
5. X-ray data at low redshift show that clusters with FR II sources tend to be underluminous in the X-ray compared to clusters without FR II sources. This suggests that the ICM pressures in these clusters are relatively low, consistent with the results obtained from the analysis of the nonthermal pressures of FR II sources.
6. Unfortunately, the X-ray data for high-redshift clusters with FR II sources are inconclusive because of the large number of upper bounds involved and possible AGN contribution to the X-ray luminosity. However, the fact that most high-redshift FR II radio galaxies have nonthermal pressures similar to their low-redshift counterparts indicates that the gaseous environments around them are similar, in which case most high-redshift clusters with FR II sources should be underluminous X-ray emitters, as are their low-redshift counterparts.
7. Thus, the evolution in the clustering strength around FR II sources toward high-redshift is likely to be closely linked to an evolution of the state of the intracluster medium. Namely, there are more clusters of low gas pressure at high redshift, and thus more FR II sources can appear in these clusters. This is consistent with the negative evolution of the cluster X-ray luminosity function with redshift, and the fact that many high-redshift clusters have much lower X-ray luminosities than optically similar low-redshift clusters.

Subject headings: galaxies: clusters: general — galaxies: structure — intergalactic medium — radio continuum: galaxies

1. INTRODUCTION

The effect of environment on radio sources has always been an interesting problem and has been considered in a large number of studies. The close interaction between radio sources and their gaseous environments makes them appealing candidates as probes of their environments. And the evolution of radio sources closely reflect the evolution of their environments.

It has been reported that at low redshift, the low-luminosity, "edge-darkened" FR I radio sources (Fanaroff & Riley 1974) usually inhabit rich cluster environments, while the powerful "edge-brightened" FR II sources (Fanaroff & Riley 1974) tend to lie in either small groups of sub-Abell richness or isolated fields (Longair & Seldner 1979, hereafter LS79; Prestage & Peacock 1988, hereafter PP88; Yates, Miller, & Peacock 1989, hereafter YMP89; Hill & Lilly 1991, hereafter HL91). This difference between the environments of FR I and FR II sources is usually thought to be due to the fact that rich clusters contain a hot intracluster medium (ICM) whose high pressure severely disrupts the jets coming from the radio core and/or the related shocks and thus prevents the formation of the

[1] National Young Investigator.

"classical-double" FR II sources, except for sources with very high beam power, such as Cygnus A (PP88; YMP89; HL91). However, as was pointed out in PP88, there are rare yet important exceptions, namely, there are indeed FR II sources in rich clusters of galaxies at low-redshift, some of which are of moderate radio power as opposed to the very high radio power of Cygnus A.

More recent investigations of the cluster environments of radio sources at $z \sim 0.5$ reveal that the FR II sources at that epoch tend to inhabit optically richer environments than they do at present, while the FR I sources show no change in environment between the two epochs (YMP89; HL91; Allington-Smith et al. 1993, hereafter AS93). Similar results for radio-loud quasars, most of which have FR II morphology, have been reported by Yee & Green (1984, 1987). They found an increase of about a factor of 3 in quasar cluster richness between $z \sim 0.4$ to 0.6.

If, indeed, it is the high-pressured ICM that prevents FR II sources from forming in rich clusters at low redshift, then the change in environment of FR II sources with redshift would indicate a change of the ICM, a change of the power or pressure of FR II sources, or a combination of both. In the evolving ICM model, the ICM of some clusters at redshift of about 0.5 might be of lower pressure and thus sustain an FR II source. In the radio power evolution model, high-redshift radio sources have higher radio power than low-redshift ones and thus can survive as FR II sources in richer environments (just as Cygnus A is able to survive due to its high radio power). HL91 suggested that the evolving ICM model might be important since: (1) there is no dependence of radio power on cluster environment at $z \sim 0.5$, as was confirmed by the results in AS93; and (2) the 1 Jy and 5C 12 sources at $z \sim 0.5$ in their sample have the same power as sources at low redshift, yet they inhabit much richer environments than the low-redshift sources.

Two approaches can be taken to investigate whether the high-pressure of the ICM in rich clusters is the reason why FR II sources tend to avoid rich environments at low redshift and whether the evolution in the clustering strength around FR II sources is caused by an evolution of the state of the ICM. The first is to compare the properties of FR II sources in cluster and noncluster environments. The second is to compare clusters with and without FR II sources. Since it is the gaseous rather than the galactic environment that is assumed to affect the morphology of the radio source, the best parameter to compare between clusters with and without FR II sources is their X-ray luminosities. If the ICM in clusters containing FR II sources are of relatively low pressure, then they will have relatively low X-ray luminosities, especially if the low gas pressure is due to a low gas density.

To investigate these questions, we searched the literature and compiled a sample of FR II sources in cluster and noncluster environments, both at low ($z < 0.35$) and high ($0.35 < z < 0.7$) redshift. The radio properties of these FR II sources, as well as the optical properties of their host galaxies, were compared to search for environment-related differences. The X-ray properties of the clusters around FR II sources, wherever available, were also closely compared to different samples of X-ray clusters without FR II sources, both at low and high redshift.

The samples are described in § 2. Data and special considerations about some of the sources in our sample are presented in § 3. The properties of FR II radio galaxies in cluster and noncluster environments, both at high and low-redshift are discussed in § 4. In § 5 the X-ray properties of the clusters with and without FR II sources are compared. A summary and discussion of the primary results are presented in § 6. Values of Hubble's constant $H_0 = 100\ h$ km s^{-1} Mpc^{-1} and the de/acceleration parameter $q_0 = 0$ are adopted throughout.

2. THE SAMPLE

2.1. *FR II Radio Galaxies and Their Environments*

2.1.1. *Sample Selection*

The majority of the FR II sources in cluster and noncluster environments used here come from studies of radio sources and their environments by PP88, HL91, YMP89, and AS93. These authors classified the sources as FR II sources based on their morphology; that is, those that are edge-brightened are designated FR II. A few of the sources listed in these papers as FR I sources were later found to have FR II morphology and are included here as FR II sources, and those listed as FR II and later found to be FR I are not included here. In total, 88 FR II radio galaxies within the redshift range 0 to about 0.7 from these studies are included here; radio quasars are not included.

The FR II galaxies are divided in to several subsamples according to redshift and clustering strength. Those with richness greater than or equal to Abell class 0 are classified as being in clusters. Others with richness less than Abell 0 are categorized as being in noncluster environments. Two nearby FR II galaxies, 3C 223.1 and 3C 310, are studied by PP88 and AS93, and are shown to lie in environments that are less rich than Abell clusters. These two sources are known to lie in Zwicky clusters, which are usually clusters poorer than Abell clusters. We thus create a fifth subsample, low-redshift FR II galaxies in Zwicky clusters, as an intermediate category between FR II galaxies in rich clusters and in noncluster environments. Another nearby FR II galaxy, 3C 219, is also known to be in a Zwicky cluster and is included in the sample.

The high-redshift sample of FR II radio galaxies in rich clusters described above is complemented by another source 3C 19, which is listed in the X-ray observations of clusters of galaxies by Henry, Soltan, & Briel (1982, hereafter HSB82). Radio and X-ray observations of Abell clusters by Rudnick & Owen (1977), Burns, Owen, & Rudnick (1978), and Vallée & Bridle (1982, hereafter VB82) give three more low-redshift FR II sources in rich clusters: 0816+52 in A643, 1232+414 in A1562, and 1333+412 in A1763. X-ray and radio observations of Abell clusters by Burns et al. (1994, hereafter BROP94) show that A1425 and A1836 also contain edge-brightened doubles. Finally, the well-known source Cygnus A is also added to the sample of low-redshift FR II sources in rich clusters.

Our final sample thus consists of 17 high-redshift FR II galaxies in rich clusters, 20 high-redshift FR II galaxies in noncluster environments, 13 low-redshift FR II galaxies in rich clusters, 43 low-redshift FR II galaxies in noncluster environments, and three low-redshift FR II galaxies in Zwicky clusters.

2.1.2. *Radio, Optical, and X-Ray Data*

Zirbel & Baum (1995, hereafter ZB95) have compiled a large sample of radio sources with radio and optical information. There is significant overlap between the sample

defined above and that of ZB95. For the overlap sources, information on the radio power at 408 MHz (P_{408}), core radio luminosity at 5 GHz ($P_{c,5\ \mathrm{GHz}}$), emission-line luminosity (L_{em}), and absolute V magnitude (M_V) are taken from ZB95; P_{408} and $P_{c,5\ \mathrm{GHz}}$ for sources not in ZB95, as well as other radio information such as linear sizes and radio maps for all sources are taken from various references, which are listed in § 3.

Most X-ray luminosities for sources in our sample are taken from five major references: HSB82, VB82, BROP94, Fabbiano et al. (1984), and Feigelson & Berg (1983, hereafter FB83), which are mostly X-ray surveys of optical clusters or radio galaxies. Detailed references for each source are listed with the data in § 3.

2.2. *Clusters without FR II Sources*

The X-ray properties of clusters with and without FR II sources will be compared. Here we describe the comparison samples of clusters without FR II sources.

2.2.1. *Low-Redshift Clusters without FR II Sources*

The properties of clusters with FR II sources are compared to clusters from the samples of Abramopoulos & Ku (1983, hereafter AK83) and HSB82 separately; since FR II sources are rare, most of these clusters do not contain FR II sources. This is done to minimize the impact of selection effects that might depend on the particular comparison sample used. Analyses using either sample yields similar results (see § 5 for more details). Thus, selection effects do not appear to be significant for the low-redshift sample.

AK83 studied the X-ray properties of 74 Abell clusters with $0 < z < 0.35$. Searching through the literature, we found radio properties for 43 of these clusters. Only two of the clusters, A1213 and A1425, contain FR II sources; FR II sources are absent from the other 41 clusters. Radio information was not available for the remaining 31 clusters. Since FR II sources rarely appear in rich clusters at low redshift, it is most likely that most of these clusters do not have FR II sources, and the results presented here are not likely to be significantly affected should a few of them turn out to contain FR II sources. The final low-redshift sample of clusters without FR II sources consists of 72 clusters; the original 74 minus the two known to contain FR II sources.

An additional 33 low-redshift clusters with $0 < z < 0.35$ are listed in HSB82; most of these are Abell clusters. The radio properties of these clusters appear to be less well studied in the literature; four of them are in the BROP94 radio survey of rich clusters of galaxies. None of these four clusters contain FR II sources. All 33 clusters are used for the low-redshift comparison sample, since it is likely that only a small number of these, if any, contain FR II sources.

Two clusters, A348 and A586, are listed by both AK83 and HSB82. Unfortunately, there are discrepancies between the X-ray luminosities listed in the two papers. The X-ray luminosity in the energy band 0.5–2 keV for A348 is $2.4 \times 10^{43}\ h^{-2}$ ergs s^{-1} in HSB82, and is $3.3 \times 10^{43}\ h^{-2}$ ergs s^{-1} in AK83. For A586, HSB82 gave an X-ray luminosity of $7.0 \times 10^{43}\ h^{-2}$ ergs s^{-1}, while AK83 set an upper limit of $2.3 \times 10^{43}\ h^{-2}$ ergs s^{-1}; the cause of the discrepancies is unclear.

However, a comparison of the two samples shows that there is not a significant difference between them. The X-ray luminosities of the two samples span about the same range (see Figs. 10 and 11 below), and the average and median X-ray luminosities of the two samples are similar (see Table 9 below for numerical values). The slightly higher $L_{X(\mathrm{mean})}$ for the HSB82 sample is probably a result of the fact that the fraction of clusters with richness class greater or equal to Abell 2 is higher in HSB82 than that in AK83.

2.2.2. *High-Redshift Clusters without FR II Sources*

The high-redshift sample of clusters without FR II sources contains 26 clusters with redshifts in the range of 0.35 to 0.60; 15 of them are from in HSB82, 10 are from the X-ray EMSS survey (Gioia et al. 1990; Henry et al. 1992, hereafter H92; Gioia & Luppino 1994), and two are from Sokoloski, Daly, & Lilly (1996). This adds up to 26 clusters since CL 0016+1609 is in both HSB82 and EMSS; the X-ray luminosity of this source listed in each sample agrees to within about 20%. The EMSS is an X-ray survey, while HSB82's sample clusters are either optically or radio selected. Nonetheless, the average X-ray properties of the samples seems to be quite similar, as discussed below.

The mean X-ray luminosity for the 15 high-redshift clusters without FR II sources in HSB82, including seven upper bounds as detections, is $L_X = (5.11 \pm 1.91) \times 10^{43}\ h^{-2}$ ergs s^{-1}, and the median X-ray luminosity is $2.6 \times 10^{43}\ h^{-2}$ ergs s^{-1}. The average X-ray luminosity is dominated by one very X-ray bright cluster: 0016+1609. The mean X-ray luminosity for the 14 clusters other than 0016+1609 is $L_X = (3.33 \pm 0.75) \times 10^{43}\ h^{-2}$ ergs s^{-1}, and the median X-ray luminosity is $2.3 \times 10^{43}\ h^{-2}$ ergs s^{-1}. For the 10 high-redshift clusters without FR II sources in EMSS, the average X-ray luminosity is $L_X = (11.15 \pm 3.31) \times 10^{43}\ h^{-2}$ ergs s^{-1}, and the median X-ray luminosity is $7.90 \times 10^{43}\ h^{-2}$ ergs s^{-1}. The average X-ray luminosity is dominated by two very X-ray bright clusters: 0016+1609 and 0451.6−0305. Without the two clusters, the mean X-ray luminosity is $L_X = (6.46 \pm 1.05) \times 10^{43}\ h^{-2}$ ergs s^{-1}, and the median X-ray luminosity is $7.50 \times 10^{43}\ h^{-2}$ ergs s^{-1}.

Thus, it appears that the EMSS clusters are more X-ray luminous than the HSB82 clusters. More specifically, while the most luminous X-ray clusters in HSB82 and EMSS have comparable X-ray luminosities, clusters with very low X-ray luminosities are missing in the EMSS, as is expected for an X-ray selected sample.

In order to make sure that this selection effect does not strongly influence the results, analyses with and without the EMSS clusters are studied. The basic results are similar (see § 5 for more detail.)

2.3. *Selection Effects*

The samples of FR II sources come from different surveys and do not constitute a statistically complete sample. Nevertheless, constructing and studying a relatively large sample may indicate some useful trends. Furthermore, most FR II sources in our sample come from studies of environments of unbiased samples of radio sources. The properties of the radio sources, as well as the properties of their environments, span large ranges, and are not biased in any obvious way. They are likely to be *representative* samples of FR II sources in different environments.

There is a selection effect that remains important for our sample. A large portion of the radio galaxies studied here come from the flux-limited 3C sample, although several sources from deeper surveys (e.g., B2 survey) are also included. As a result, trends of source characteristics with redshift could be affected by the fact that higher redshift

sources are intrinsically more powerful radio sources on average (see § 4.1 for more discussion). However, this redshift-related selection effect does not affect comparison between radio galaxies at a given redshift in different environments, since cluster and noncluster sources are equally affected by this bias.

Most X-ray luminosities of clusters with FR II sources come from X-ray studies of optical clusters or radio galaxies. These X-ray luminosities are compared with those of clusters without FR II sources, some of which are optically selected (AK83 and HSB82), radio selected (HSB82), or X-ray selected (EMSS), as described in § 2.2. No obvious selection effects are expected in the X-ray comparison except, possibly, for the comparison with the EMSS clusters, which are discussed in § 2.2.2. A comparison of AK83 and HSB82 do not indicate serious selection effects, as discussed in § 2.2.1. Furthermore, X-ray comparison of clusters with and without FR II sources yield similar results no matter which comparison sample is used (see § 5 for details). Thus, although no statistically significant conclusion can be made before a more complete sample is available, the general trends seen in the present sample are likely to be fairly reliable.

3. DATA AND SPECIAL CONSIDERATIONS

3.1. *Data*

3.1.1. *FR II Radio Galaxies in Noncluster Environments*

Radio, optical, and X-ray data for FR II sources in noncluster environments at low and high redshift are listed in Tables 1 and 2, respectively. The meaning of each column is as follows.

Column (1).—The name of the source.

Column (2).—The IAU name of the source.

Column (3).—The redshift of the source.

Column (4).—The largest linear extent of the radio source, D, in unit of h^{-1} kpc, taken to be the separation of the outmost peaks of surface brightness (i.e., hot spot separation).

Column (5).—The logarithm of the 408 MHz radio luminosity density in units of h^{-2} ergs s^{-1} Hz^{-1}.

Column (6).—The logarithm of the 5 GHz radio nuclear luminosity density in unit of h^{-2} ergs s^{-1} Hz^{-1}.

Column (7).—The logarithm of the emission-line luminosity of the host galaxy in h^{-2} ergs s^{-1}, taken from ZB95 with proper adjustment of cosmology.

Column (8).—The rest frame V magnitude of the host galaxy taken from ZB95 with proper adjustment of cosmology.

Column (9).—The minimum-energy magnetic field of the radio bridge of the FR II source in unit of 10^{-5} $h^{2/7}$ G. Published radio maps were found for 33 of the sources listed in Tables 1, 2, 3, 4, and 5, and 29 of these maps were high-resolution maps. When a high-resolution map is available, the magnetic field is estimated at several points along the ridge line of the bridge, excluding regions that are too close to the hot spot or radio core. In most cases, 25 h^{-1} kpc from either location is allowed. The bridge field is taken to be the average of the field measured at several points along the bridge. The standard formula from Miley (1980) is used with the following assumptions: the ratio between the energy of electrons and heavy particles is 1; the radio spectrum is a power law from 10 MHz to 100 GHz; the volume filling factor is 1; and the source is randomly oriented relative to the observer (the line of sight depth is taken as $4/\pi$ times the source width). Published radio maps and mean spectral index for each source are used. The radio surface brightness is taken directly from the radio map, and the bridge width is estimated assuming that locally the bridge is cylindrically symmetric with constant volume emissivity; of course, Gaussian smearing with a beam given by that used to observe the source is accounted for, as described in § 4.2.3.

For the four sources without high-resolution bridge maps, an average magnetic field strength over the sources is estimated by dividing the total radio power by the total radio emitting volume including the radio hot spots and bridge assuming that the bridge extends to the radio core; field strengths estimated in this way are marked by an asterisk (which is relevant for Tables 3 and 4). Average $B_{\rm min}$ is calculated using the standard formula from Pacholczyk (1970) with the same parameters described above.

Due to the uncertainties in the assumptions used and the large error involved in estimating the volume of the radio galaxy, the error in the values of the $B_{\rm min}$ is rather large; a typical number is $\sim$30%.

Column (10).—The nonthermal pressure in the radio source in units of 10^{-11} $h^{4/7}$ dyne cm^{-2}. The nonthermal pressure $P_{\rm nth}$ is a third of the energy density u, and the total energy density is taken to be that under the minimum energy condition: $P_{\rm nth} = (1/3)u_{\rm min} = 1/3(B^2_{\rm min}/8\pi) \times 7/3 = (7/72\pi)B^2_{\rm min}$. If the B field strength is either greater or less than $B_{\rm min}$, the nonthermal pressure will be greater than that listed here.

Column (11).—X-ray luminosity in the energy band 0.5–2 keV in unit of 10^{43} h^{-2} ergs s^{-1};

Column (12).—References for each source.

3.1.2. *FR II Radio Galaxies in Clusters*

The same parameters listed in Tables 1 and 2 are listed in Tables 3, 4, and 5 for FR II sources in low-redshift rich clusters, high-redshift rich clusters, and low-redshift Zwicky clusters respectively. Two additional columns of information are included in these tables, as described below.

Column (12).—The number density of electrons at the center of the cluster in unit of 10^{-3} $h^{1/2}$ cm^{-3}. This has been estimated by assuming that the cluster gas is described by a King model with $\beta = \frac{2}{3}$, typical for low-redshift galaxy clusters (cf. Jones & Forman 1984). Thus, the X-ray luminosity of the cluster is

$$L_{\rm X} = 1.968 \times 10^{-26} g n_0^2 (e^{-E_1/kT} - e^{-E_2/kT}) a_c^3 T^{1/2} \text{ ergs s}^{-1} ,$$

where all parameters are in cgs units and where a_c is the core radius of the cluster, g is the integrated Gaunt factor, T is the temperature of ICM, and E_1 and E_2 are the lower and upper limits to the energies between which the X-ray luminosity is calculated; here, $E_1 = 0.5$ keV and $E_2 = 2$ keV have been adopted. The central density is estimated given the X-ray luminosity and assuming $g = 1.2$, $T = 6$ keV, and $a_c = 0.2\ h^{-1}$ Mpc unless there are observed values for these quantities. For sources that are offset from the center of the cluster, the number density at the position of the radio source estimated using the same model is also listed and is denoted as (R). High-redshift FR II sources in clusters are assumed to lie within the cluster core.

Column (13).—The thermal pressure corresponding to n_0 in unit of 10^{-11} $h^{1/2}$ dyne cm^{-2}: $P_{\rm th} \simeq 2n_0\, kT$.

TABLE 1

LOW-REDSHIFT FR II SOURCES IN NONCLUSTER ENVIRONMENTS

Name (1)	IAU (2)	z (3)	D (4)	P_{408} (5)	$P_{c5\,GHz}$ (6)	L_{em} (7)	M_V (8)	B_{min} (9)	P_{nth} (10)	L_X (11)	References (12)
3C 17	0035−024	0.22	71.6	33.88	32.51	...	−20.89	...	...	...	5, 47, 51, 52
3C 33	0106+130	0.060	199.1	33.07	29.98	41.39	−20.90	0.65	0.13	<0.006	5, 17, 26, 30, 34, 37, 43, 44, 50, 52
3C 63	0218−021	0.175	...	33.58	30.71	41.87	−21.24	...	...	...	5, 52
3C 67	0221+28	0.310	7.6	33.91	32.54	42.75	−21.32	...	...	...	5, 34, 37, 52
3C 88	0325+02	0.030	84.5	31.98	30.21	40.45	−21.06	...	...	0.0201	18, 34, 43, 44, 50, 52
3C 98	0356+10	0.031	129.2	32.42	28.96	40.57	−20.44	0.9	0.25	0.0101	5, 17, 18, 26, 31
.....											32, 34, 37, 43, 44, 50, 52
3C 105	0404+03	0.089	352.1	32.96	30.08	40.57	−19.32	...	...	...	5, 34, 43, 44, 52
3C 109	0411+11	0.306	288.6	34.14	32.61	42.81	−22.53	...	...	16.80	5, 17, 26, 37, 50, 52
3C 184.1	0734+805	0.118	260.1	33.08	29.98	42.22	−20.69	0.8	0.20	0.21	5, 17, 26, 30, 31, 32, 34, 37, 52
3C 192	0802+24	0.060	151.9	32.64	29.44	41.11	−20.43	0.9	0.25	0.0439	17, 26, 31, 32, 37, 43, 44, 52
3C 198	0819+06	0.081	209.9	32.63	...	...	−20.19	...	...	...	5, 34, 43, 44, 52
3C 223	0936+361	0.137	477.3	33.25	30.30	39.75	−21.07	0.65	0.13	0.272	5, 17, 26, 30, 31, 32, 34, 37, 50, 52
3C 227	0945+07	0.086	237.7	33.17	30.20	42.02	−20.69	...	...	...	5, 34, 43, 44, 52
3C 236	1003+35	0.099	3000.7	33.02	31.23	40.91	−21.29	...	...	...	5, 26, 34, 37, 43, 44, 50, 52
3C 277.3	1251+27	0.086	35.4	32.67	30.14	...	−21.04	...	...	<0.1361	5, 17, 26, 34, 37, 43, 44, 52
3C 287.1	1330+022	0.216	275.3	33.48	...	...	−21.18	...	...	...	5, 34, 47, 52
3C 293	1350+31	0.045	132.3	32.36	30.34	41.24	−21.33	...	...	0.0252	17, 26, 28, 34, 37, 43, 44, 52
3C 303	1441+522	0.141	53.9	33.16	31.53	41.57	−20.92	...	...	2.0165	5, 17, 26, 30, 34, 37, 47, 52
3C 320	1530+36	0.342	58.2	33.91	...	...	−21.64	3.1	3.0	...	5, 7, 34, 52
3C 321	1529+24	0.096	353.0	32.94	30.50	42.12	−21.86	...	...	<0.2185	5, 17, 26, 28, 34, 37, 43, 44, 50, 52
3C 326	1549+202	0.090	1346.1	32.90	30.06	<39.97	...	...	...	<0.0655	5, 17, 26, 34, 52
3C 332	1615+324	0.152	163.0	33.09	30.38	...	−21.44	...	...	...	5, 31, 34, 52
3C 348	1648+050	0.154	208.2	34.66	30.48	...	−21.76	...	...	4.0717	18, 34, 51, 52
3C 381	1832+474	0.161	129.5	33.43	30.22	41.36	−21.32	1.3	0.52	<0.3025	5, 17, 26, 30, 34, 37, 50, 52
3C 390.3	1845+79	0.057	159.8	32.96	31.09	42.27	−20.84	0.7	0.15	4.309	5, 17, 26, 30, 34, 37, 43, 44, 50, 52
3C 434	2120+155	0.322	37.3	33.61	...	...	−21.05	...	...	...	5, 34, 51, 52
3C 445	2221−02	0.056	...	32.64	30.50	41.85	−20.67	...	...	...	5, 43, 44, 50, 52
3C 452	2243+39	0.081	262.1	33.33	30.96	41.12	−21.12	...	...	<0.2521	17, 18, 26, 34, 37, 43, 44, 50, 52
3C 458	2310+030	0.289	466.9	33.94	...	42.42	...	...	...	...	34, 51, 52
3C 459	2314+038	0.220	19.6	33.93	32.86	41.84	−21.67	...	...	...	5, 34, 52
4C 18.06	0124+18	0.043	...	...	...	...	...	...	...	...	43, 44
4C 32.25	0828+32	0.051	220.2	32.08	28.96	...	...	...	...	...	34, 43, 44, 52
4C 36.47	2244+36	0.081	18.0	...	...	...	...	...	...	...	34, 43, 44
4C 37.29	1107+379	0.346	267.0	33.88	...	...	−21.08	1.3	0.52	...	5, 23, 34, 52
4C 73.08	0945+73	0.058	604.5	32.48	29.87	40.85	...	...	...	...	34, 43, 44, 52
PKS	0043−424	0.053	...	32.67	...	...	−20.29	...	...	...	5, 52
PKS	0114−476	0.146	1005.6	33.26	...	...	−22.03	...	...	...	5, 34, 52
PKS	0229+034	0.273	...	...	...	...	−20.98	...	...	...	5, 52
PKS	0349−278	0.066	322.7	32.88	29.82	40.79	−20.99	...	...	...	5, 34, 52
PKS	0518−458	0.035	203.1	33.26	31.14	40.98	−19.70	...	...	...	5, 34, 50, 52
PKS	1331−099	0.081	811.4	32.66	...	...	−21.27	...	...	...	5, 34, 52
	1514+00	0.053	...	...	...	...	...	...	...	...	43, 44
DA240	0744+55	0.036	1012.4	32.22	30.39	39.4	...	...	...	<0.0304	18, 34, 43, 44, 50, 52

REFERENCES.—(1) Abramopoulos & Ku 1983; (2) Akujor et al. 1990; (3) Akujor et al. 1994; (4) Allington-Smith 1982; (5) Allington-Smith et al. 1993; (6) Arnaud et al. 1984; (7) Bondi et al. 1993; (8) Burns et al. 1978; (9) Burns et al. 1981; (10) Burns & Gregory 1982; (11) Burns et al. 1994; (12) Carilli et al. 1991; (13) Carilli et al. 1994; (14) Clarke et al. 1992; (15) Eales 1985; (16) Fabbiano et al. 1979; (17) Fabbiano et al. 1984; (18) Feigelson & Berg 1983; (19) Fernini et al. 1993; (20) Henry et al. 1982; (21) Hill & Lilly 1991; (22) Jenkins et al. 1977; (23) Gregorini et al. 1988; (24) Burns et al. 1984; (25) Laing 1981; (26) Laing et al. 1983; (27) Law-Green et al. 1995; (28) Leahy & Williams 1984; (29) Leahy et al. 1989; (30) Leahy & Perley 1991; (31) Miller 1985; (32) Miller et al. 1985; (33) Morganti et al. 1988; (34) Nilson et al. 1993; (35) Owen 1976 ; (36) Owen 1975; (37) Peacock & Wall 1981; (38) Parma et al. 1986; (39) Parma et al. 1991; (40) Parma et al. 1987; (41) Perley et al. 1980; (42) Pooley & Henbest 1974; (43) Prestage & Peacock 1988; (44) Prestage & Peacock 1989; (45) Riley 1975; (46) Rudnick & Owen 1977; (47) Signal 1993; (48) Vallée & Bridle 1982; (49) van Breugel et al. 1984; (50) Wall & Peacock 1985; (51) Yates et al. 1989; (52) Zirbel & Baum 1995.

3.1.3. *Low-Redshift Clusters without FR II Sources*

In Table 6 the mean X-ray luminosities for the two samples of low-redshift clusters without FR II sources, AK83 and HSB82, are listed (see § 2.2.1). The meaning of each column is as follows: (1) range of L_X; (2) average L_X; (3) median L_X; (4) total number of clusters; and (5) the number of upper bounds on L_X; these have been included as detections.

3.1.4. *High-Redshift Clusters without FR II Sources*

The data relevant for the high-redshift clusters without FR II sources are listed in Table 7. Listed in the columns are: the cluster name (col. [1]), X-ray luminosity in the 0.5–2 keV energy band (col. [2]), redshift (col. [3]), and richness in terms of Abell class (col. [4]). The two clusters from Sokoloski et al. (1994, 1996), 53W076 and 53W080, are listed first, followed by the 10 clusters from the EMSS and then by the 14 clusters from HSB82. Two values of X-ray luminosity are given for 0016+1609; one from HSB82, denoted HSB82, and one from Gioia & Luppino (1994), denoted EMSS.

3.2. *Special Considerations*

3.2.1. *AGN Contribution to L_X*

It has long been recognized that active galactic nuclei (AGNs) in radio galaxies can produce a significant amount of X-ray emission. Determining whether the X-ray emission from a cluster that contains a radio galaxy is from the

TABLE 2

HIGH-REDSHIFT FR II SOURCES IN NONCLUSTER ENVIRONMENTS

Name (1)	IAU (2)	z (3)	D (4)	P_{408} (5)	$P_{c5\,GHz}$ (6)	L_{em} (7)	M_V (8)	B_{min} (9)	P_{nth} (10)	L_X (11)	References[a] (12)
3C 16.....	0035+130	0.405	215.2	33.96	<30.13	...	−20.73	1.8	1.0	...	5, 26, 30, 34, 51, 52
3C 42.....	0126+29	0.395	98.9	34.20	30.82	41.46	−21.03	2.8	2.4	...	5, 26, 30, 34, 37, 52
3C 200	0824+29	0.458	92.4	34.29	32.09	...	−21.05	...	...	1.8	5, 20, 21, 26, 34, 52
3C 225.0B.....	0939+139	0.582	21.4	34.76	...	...	...	...	...	...	26, 34, 37, 51
3C 274.1	1232+21	0.422	551.0	34.38	31.43	...	−20.91	1.2	0.45	...	5, 21, 26, 28, 34, 51, 52
3C 275	1239−044	0.480	...	34.44	...	42.70	−21.25	...	...	...	5, 21, 51, 52
3C 299	1419+42	0.367	...	34.10	31.96	42.92	−21.30	...	...	...	5, 21, 26, 37, 52
3C 306.1	1452−041	0.442	350.2	34.29	...	42.64	−21.37	...	...	...	5, 21, 47, 51, 52
3C 327.1	1602+14	0.463	62.0	34.81	32.37	42.24	...	...	...	...	34, 51, 52
3C 341	1626+28	0.448	311.7	34.21	30.45	42.32	−20.75	2.3	1.6	...	5, 21, 26, 30, 34, 52
3C 457	2309+18	0.428	703.7	34.22	...	...	−20.67	0.95	0.28	...	5, 26, 30, 34, 52
4C 34.42	1539+34	0.402	224.9	34.25	...	...	−21.66	0.92	0.26	...	5, 23, 34, 52
5C 12.217	1301+34	0.428	...	32.48	...	...	−20.55	...	...	...	5, 21, 52
5C 12.241	1302+36	0.487	...	33.29	...	...	−20.64	...	...	...	5, 21, 52
PKS	0101+023	0.390	...	33.53	...	...	−20.98	...	...	...	5, 52
B2	0822+34A	0.406	64.7	33.58	...	...	−20.82	...	...	...	4, 5, 15, 21, 34, 52
B2	1025+39	0.36	6.7	34.21	...	...	−21.56	...	...	...	4, 5, 15, 52
B2	1104+36	0.393	70.5	33.55	...	...	...	...	...	...	4, 5, 15, 21
B2	1201+39	0.445	11.4	33.47	...	...	−21.01	...	...	...	4, 5, 15, 21, 52
B2	1301+38A	0.47	109.3	33.69	...	...	...	...	...	...	4, 5, 15, 21, 34

[a] See reference list in Table 1.

galaxy or the cluster is often impossible without a resolved X-ray map, high-sensitivity spectral information, or variability information. In practice, neither X-ray variability or spectral information is detailed enough to be useful, and the resolution of the X-ray emission is often the primary way to distinguish pointlike from extended X-ray emission. Unfortunately, at high redshift, none of the clusters containing FR II sources are spatially resolved in the X-ray except for 3C 295.

At low redshift, out of the nine clusters with FR II sources that have X-ray data, only the X-ray emission from Cygnus A and 1333+412 are clearly extended emission from the ICM. X-ray emission in the vicinities of 3C 388, 4C 29.41 appear to be extended, but are not well resolved. For the Abell cluster A1836, there is a weak X-ray detection of the AGN associated with the FR II radio galaxy in it and possibly extended X-ray emission as well (cf. BROP94). None of the remaining four clusters with FR II sources are resolved.

Out of the three low-redshift FR II sources in Zwicky clusters, only 3C 310 appears to be extended, but nearly all the X-ray flux comes from an unresolved core; the other two are not resolved.

It is thus important to consider X-ray emission from the AGNs in all but the Cygnus A and 1333+412 clusters.

A strong correlation between X-ray luminosity and 5 GHz radio nuclear luminosity is reported by Fabbiano et al. (1984) for FR II radio galaxies. Fabbiano et al. (1984) interpret this to mean that the X-ray emission arises from the nuclear region of the radio galaxy.

To see whether the X-ray emission from the vicinity of FR II radio galaxies might originate from the AGN, the X-ray luminosities of FR II radio galaxies (in all environments) are plotted versus 5 GHz radio core luminosity in Figure 1; the data are taken from Tables 1–5. FR II sources from the Fabbiano et al. (1984) sample are also shown in the figure and are denoted by crosses.

The locus of points defined by the FR II sample considered here is similar to that defined by the Fabbiano et al. (1984) sources. Thus, the X-ray emission detected from the vicinity of the FR II sources considered here could be produced by the AGN. The fact that Cygnus A and 3C 295, whose X-ray luminosities are dominated by X-ray emissions from the ICM, follow the same trend as other FR II sources shows that the conclusions that can be drawn from Figure 1 are quite limited; the X-ray emission could arise either from the AGN or from the ICM. The trends seen in Figure 1 do imply that X-ray emission from AGN can have a luminosity comparable to that of the cluster ICM.

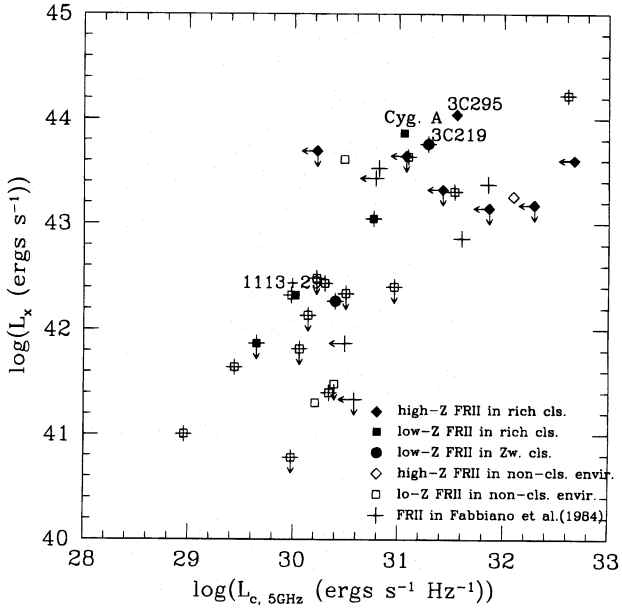

FIG. 1.—The logarithm of the X-ray luminosity in the energy band 0.5-2 keV in units of h^{-2} ergs s^{-1} vs. the 5 GHz radio core luminosity in units of h^{-2} ergs s^{-1} Hz^{-1} for FR II radio galaxies in this study (in all environments) and for the FR II radio galaxies which are in Fabbiano et al. (1984).

TABLE 3

LOW-REDSHIFT FR II SOURCES IN RICH CLUSTER ENVIRONMENTS

Name	IAU	z	D	P_{408}	P_{cbG}	L_{em}	M_v	B_{min}	P_{nth}	L_x	n_0	P_{th}	ref[1]
1	2	3	4	5	6	7	8	9	10	11	12	13	14
3C285	1319+42	0.079	137.4	32.55	29.65	41.15	-20.95	0.65	0.13	<0.0739	< 0.28	<0.54	17,26,28,34,43,44,52,
3C388	1842+45	0.091	36.0	33.10	30.76	40.32	-22.56	2.2	1.5	1.1091	1.0	2.0	17,18,25,26,34,37,39,42,43,44,50,52,
3C405[2] (Cyg. A)	1957+40	0.056	93.1	35.23	31.05	41.77	-21.51	5.43	9.1	7.31	9.9	21	6,12,13,16,28,29,52,
4C29.41[3] (A1213)	1113+29	0.048	51.7	32.10	30.02	40.27	...	1.0	0.31	0.21	2.4(C) 0.94(R)	4.6(C) 1.8(R)	1,33,34,35,36, 38,39,40,45,52,43,44,
4C29.44	1152+30	0.329	57.5	33.93	...	...	-21.55	3.5	3.8	...	...	...	5,7,34,52,
PKS	0211-479	0.22	801.3	...	...	...	...	...	...	...	...	...	34,51,
PKS	0511-48A	0.306	...	...	...	...	...	...	...	...	...	...	51,
PKS	1928-340	0.098	...	32.61	...	...	-22.12	...	...	...	...	...	5,52,
B3[4] (A1763)	1333+412	0.189	25.5	33.16	...	...	...	4.1*	5.2*	15.7	2.6	5.0	34,35,36,46,48,
... (A643)	0816+52	0.138	52.3	33.04	...	...	...	2.3	1.6	<0.13	<0.37(C) <0.12(R)	<0.71(C) <0.23(R)	8,35,36,46,48,
... (A1562)	1232+414	0.170	165.2	32.74	...	...	...	0.9	0.25	<0.26	<0.11	<0.21	35,36,46,48,
...	A1425	0.1120	...	32.71	...	...	...	...	...	<0.051	<0.23	<0.45	1,11,
...	A1836	0.0365	...	31.89	...	...	...	...	...	0.0086	0.096	0.18	11,

[1] See the reference list in Table 1.
[2] $a_c = 70\,h^{-1}$ kpc.
[3] $a_c = 270\,h^{-1}$ kpc.
[4] $a_c = 96\,h^{-1}$ kpc; $kT = 6.5$ keV.
* B_{min} is $B_{average}$ rather than B_{bridge}.

1996ApJ...467..145W

TABLE 4

HIGH-REDSHIFT FR II SOURCES IN RICH CLUSTER ENVIRONMENTS

Name	IAU	z	D	P_{408}	P_{cbG}	L_{em}	M_v	B_{min}	P_{nth}	L_w	n_0	P_{th}	ref[1]
1	2	3	4	5	6	7	8	9	10	11	12	13	14
3C19	0038+328	0.482	38.0	34.34	<32.67	...	...	4.0*	5.0*	4.0	2.1	4.0	20,22,26,34,37,52,
3C228	0947+148	0.552	191.3	34.71	31.85	43.44	...	3.0	2.8	...	...	...	21,24,26,34,37,51,52,
3C244.1	1030+58	0.428	196.3	34.45	<30.22	42.68	-21.42	2.3	1.6	<4.90	<2.3	<4.4	5,18,21,22,25,26,28,34,37,52,
3C268.3	1203+64	0.371	4.4	34.10	<32.29	42.18	-19.97	19.5*	118*	<1.5	<1.3	<2.4	5,20,21,22,26,34,37,42,49,50,52,
3C295	1409+52	0.4614	16.6	35.18	31.55	41.83	-22.48	33.8	350	11	3.4	6.6	2,3,5,20,21,22,25,26,34,37,42,50,52,
3C313	1508+08	0.461	502.2	34.53	<30.36	42.96	-21.10	...	...	...	...	...	5,21,34,52,
3C330	1609+06	0.549	237.6	34.86	<31.86	43.44	-22.59	2.4	1.8	<1.4	<1.2	<2.3	20,21,22,25,26,29,34,37,50,52,
3C435	2126+073	0.471	125.1	34.30	...	43.17	-21.14	...	...	...	...	...	5,47,51,
5C6.142	0213+33	0.448	...	32.40	...	...	-21.68	...	...	...	...	...	5,52,
5C12.75	...	0.62	...	...	...	...	...	...	...	...	...	...	21,
5C12.91	1251+37	0.464	...	32.36	...	...	-21.48	...	...	...	...	...	5,21,52,
5C12.142	...	0.65	...	...	...	...	...	...	...	...	...	...	21,
5C12.235	...	0.66	...	...	...	...	...	...	...	...	...	...	21,
B2	0847+37	0.407	118.7	33.43	...	...	-21.24	...	...	...	...	...	4,5,15,21,52,
B2	0854+39A	0.528	681.4	33.73	...	...	...	0.5	0.078	...	...	...	4,15,21,27,34,
B2	1130+34	0.512	318.9	33.85	<31.07	...	...	0.7	0.150	<4.4	<2.2	<4.2	4,15,21,27,34,
B2	1245+34	0.409	21.6	33.41	<31.42	...	-20.99	3.0*	2.8*	<2.1	<1.5	<2.9	4,5,15,21,47,52,

[1] See the reference list in Table 1.

* B_{min} is $B_{average}$ rather than B_{bridge}.

TABLE 5

LOW-REDSHIFT FR II SOURCES IN ZWICKY CLUSTERS

Name	IAU	z	D	P_{408}	P_{cbG}	L_{em}	M_v	B_{min}	P_{nth}	L_w	n_0	P_{th}	ref[1]
1	2	3	4	5	6	7	8	9	10	11	12	13	14
3C219	0917+45	0.1745	319.1	33.91	31.28	41.84	-21.70	1.0	0.31	5.75	2.5	4.7	14,17,26,32,34,37,41,50,52,
3C223.1	0938+399	0.108	157.7	32.71	...	...	-21.16	...	...	<0.172	...	...	5,9,10,34,52,
3C310	1502+26	0.054	152.4	32.86	30.40	...	-20.59	...	...	0.1848	...	...	5,9,10,17,26,28,34,37,43,44,50,52,

[1] See the reference list in Table 1.

TABLE 6

X-RAY DATA FROM AK83 AND H82

Abell Class	$L_{X(0.5-2\ keV)}$ ($10^{43}\ h^{-2}$ ergs s^{-1})	$\bar{L}_X$ ($10^{43}\ h^{-2}$ ergs s^{-1})	$L_{X(med)}$ ($10^{43}\ h^{-2}$ ergs s^{-1})	N_{cls}	$N_{upper\ bounds}$
AK83:					
0.....	0.12–10.5	1.78 ± 0.37	0.84	37	16
1.....	0.16–8.75	1.96 ± 0.48	1.33	19	2
2.....	0.38–20.0	5.27 ± 1.54	2.16	13	1
3.....	<2.31	...	...	1	1
4.....	2.17–7.47	4.82 ± 2.65	...	2	0
0–4.....	0.12–20.0	2.55 ± 0.39	1.33	72	20
H82:					
0–4.....	0.15–13	3.75 ± 0.66	2.0	33	6

Thus, it is important to keep in mind that the X-ray luminosities observed from unresolved clusters with FR II sources may have significant contribution from AGN emission, and the ICM in these clusters could have an X-ray luminosity well below observed values.

3.2.2. *Special Sources*

One FR II source in the high-redshift sample of FR II sources in rich clusters, 3C 268.3, has an extremely small linear size. This compact steep spectrum source has a linear size of merely 5 h^{-1} kpc, which means that it is almost certainly interacting with the interstellar medium (ISM) rather than the ICM. It does not really qualify as an FR II source in a cluster environment. Furthermore, cluster identification of its environ is rather dubious (cf. HL91). Thus, this source will be excluded from further analysis.

Two other high-redshift FR II sources in clusters also have relatively small linear sizes; 3C 295 has a linear size of 17 h^{-1} kpc; and 1245+34 has a linear size of 22 h^{-1} kpc. Thus, although we do not exclude them from our analysis, it should be kept in mind that these two sources could be interacting with the ISM rather than the ICM. Thus, the properties of the radio bridge probably do not provide an indicator of the pressure of the ICM.

TABLE 7

X-RAY DATA FOR HIGH-REDSHIFT CLUSTERS WITHOUT FR II

Source Name	$L_{X(0.5-2\ keV)}$ ($h^{-2}\ 10^{43}$ ergs s^{-1})	Redshift	Abell Class
53WO76	0.6	0.39	$0 \sim 1$
53WO80	8.23	0.546	>0
0016+1609	25.27 (EMSS)	0.546	3
...	30 (H82)		
0147.8−3941	2.50	0.373	...
0302.5+1717	4.68	0.425	...
0302.7+1658	8.20	0.424	...
0418.3−3844	2.24	0.350	...
0451.6−0305	34.55	0.55	...
1333.3+1725	8.94	0.460	...
1512.4+3647	7.60	0.372	...
1621.5+2640	7.39	0.426	...
2053.7−0449	10.15	0.583	...
A370.....	11	0.373	0
PKS 0116+08.....	6.0	0.594	0
A908.....	5.6	0.390	0
A913.....	5.1	0.366	1
0303+17	3.3	0.450	...
0024+1654	3.2	0.39	2
1613+31	0.89	0.415	...
1558+41	<2.6	0.580	...
1600+41	<1.9	0.54	...
A895.....	<1.5	0.36	1
0822+67	<1.5	0.384	...
2142+03	<1.4	0.550	...
0312+14	<1.3	0.510	...
0949+44	<1.3	0.385	...

4. RESULTS ON FR II SOURCES IN DIFFERENT ENVIRONMENTS

Properties of FR II sources in different environments and at different redshifts are studied in this section. Radio powers, linear sizes, and optical and emission-line properties of host galaxies of these FR II sources are compared in § 4.1. The nonthermal pressure of the radio bridge and its relationship with the thermal pressure of the surrounding medium are discussed in § 4.2.

4.1. *Radio Power, Optical, and Emission-Line Properties, and Linear Sizes*

The radio power at 408 MHz (P_{408}), the narrow emission-line luminosities (L_{em}), the absolute V magnitudes (M_V) of host galaxies, and the linear sizes of FR II sources in cluster and noncluster environments are plotted versus their redshifts in Figures 2, 3, 4, and 5, respectively. It can be seen that within each redshift bin, not only do FR II sources in different types of environments have similar radio powers, as was found by HL91 and AS93, but they also appear to have similar L_{em}, M_V, and linear sizes. These results tend to

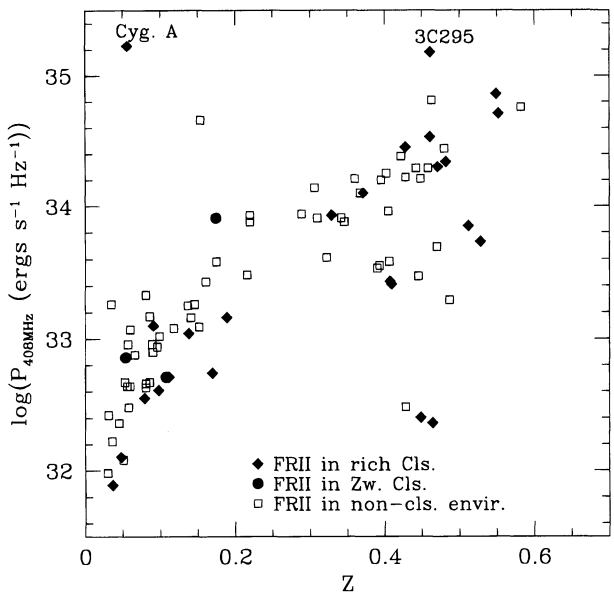

FIG. 2.—The logarithm of the total radio power at 408 MHz in units of h^{-2} ergs s^{-1} Hz^{-1} vs. redshift for FR II galaxies in different environments.

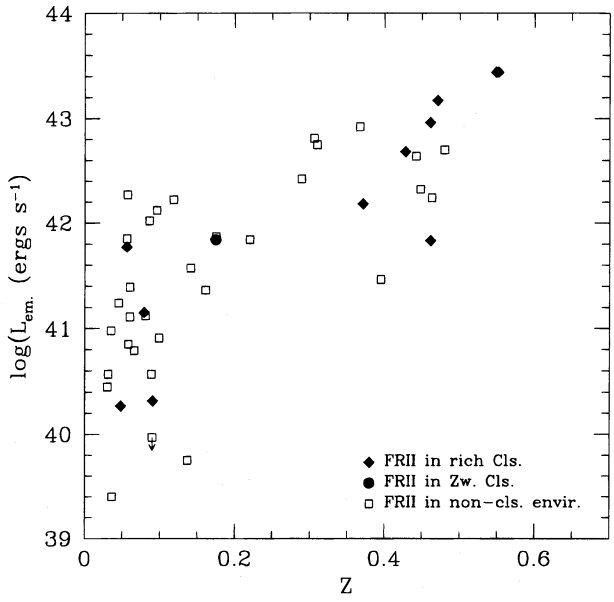

FIG. 3.—The logarithm of the narrow emission-line luminosity in units of h^{-2} ergs s^{-1} vs. redshift for FR II radio galaxies in different environments. The emission-line luminosities are taken from Zirbel & Baum (1995).

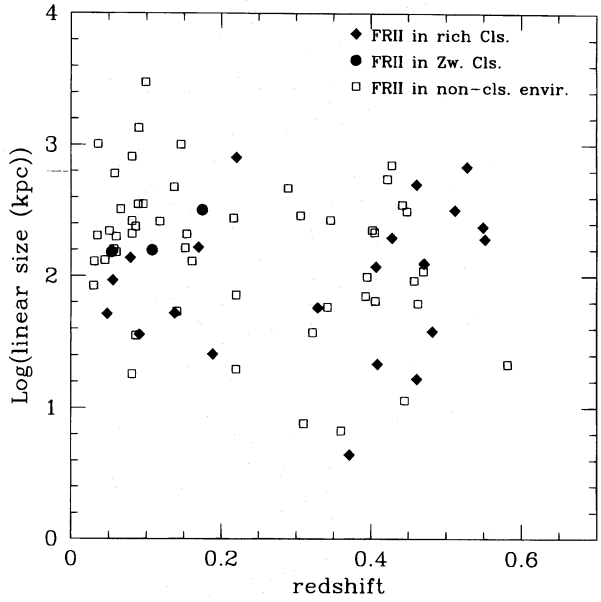

FIG. 5.—The logarithm of linear size vs. redshift for FR II radio galaxies in different environments.

suggest that, within each redshift bin, the gaseous environments around these FR II sources are similar.

Comparisons between FR II sources at high and low redshift show that high-redshift FR II radio galaxies have higher P_{408} and L_{em} values than low-redshift FR II radio galaxies on average. But there are also overlap regions. As discussed in § 2.3, many sources studied here are from the 3C sample. Thus, the increase of radio power with redshift is likely to be due to the fact that the 3C survey is flux limited. Since the emission-line luminosity is known to be correlated with the radio luminosity, both the increase of the radio power and emission-line luminosity with redshift seen in Figures 2 and 3 are likely to be due to selection effects. It is interesting to note that redshift evolution is not seen in the magnitude of the host galaxy or the linear size of the FR II source up to a redshift ~ 0.6 (see Figs. 4 and 5).

It is clear from Figures 2–5 that the richness of the optical environment does not play a role in any of the following: radio luminosity, emission-line luminosity, optical magnitude of the host galaxy, or the linear size of the radio source (as measured by the separation between the radio hot spots). That is, the sources in cluster environments, Zwicky clusters, and noncluster environments track each other quite well on these figures. Because this key result is independent of the redshift evolution of radio or emission-line luminosity, the redshift bias discussed above is unlikely to be important for this comparison.

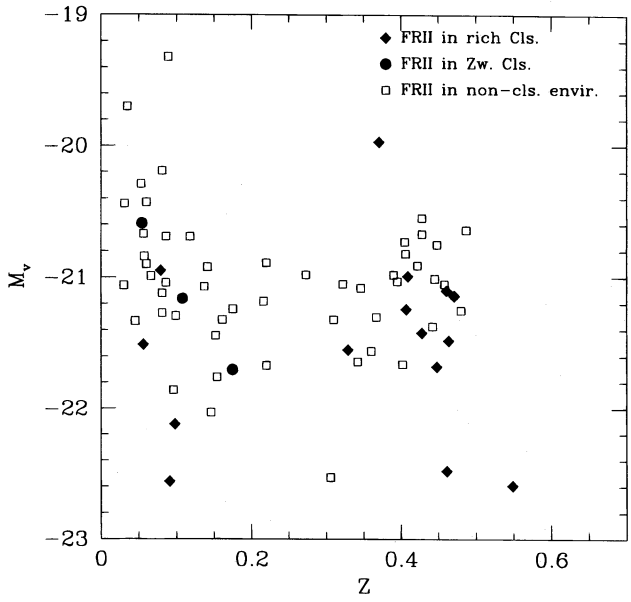

FIG. 4.—The absolute V magnitude of host galaxy vs. redshift for FR II radio galaxies in different environments. The V magnitudes are taken from Zirbel & Baum (1995).

4.2. *Nonthermal Pressure of the Radio Bridge*

4.2.1. *A Comparison with Thermal Pressure*

An important parameter is the nonthermal pressure of a radio source. Several studies of double-lobed radio sources, including both FR I and FR II sources, and their environments, such as those of Burns, Gregory, & Holman (1981) and Morganti et al. (1988), have shown that very often the external and internal pressure are on the same order, especially for relaxed radio structures. In an FR II source, the hot spots are thought to be ram pressure confined, and hence are not be thermally confined by the surrounding medium, but the radio bridges may have enough time to relax and reach pressure equilibrium with the ambient gas. Thus, it is of interest to compare the nonthermal pressure of the radio bridge and the thermal pressure of the ambient gas.

Nonthermal pressures of the radio galaxies considered here were estimated at several points along the radio bridge whenever possible. When a high-resolution map of the FR II source is available, minimum-energy magnetic field strengths (B_{min}) and nonthermal pressures (P_{nth}) are calculated at various points along the radio axis, as described in notes for column (9) in § 3.1.1. Points that are not too near to either the hot spots or the radio core are chosen so that the B field strengths calculated there are those of the bridges with little "contamination" from the hot spots and from

AGN emission. In a given source, it is found that the B field strength stays roughly constant along the bridge, with a typical variation of $\sim 30\%$. Values of $B_{\rm min}$ and P_{nth} at different points along the bridge are averaged to yield the final values of $B_{\rm min(bridge)}$ and $P_{nth(bridge)}$, which are listed in Tables 1–5.

Radio maps were available for 33 sources, and high-resolution maps were available for 29 of these. For the sources without published high-resolution maps, an average B field is estimated as described in notes for column (9) in § 3.1.1. The four sources with fields estimated in this way are marked with asterisks in Tables 1–5. The average value of the field estimated in this way is generally larger than $B_{\rm bridge}$ due to hot spot emission. For the FR II's whose $B_{\rm bridge}$ values are available, $B_{\rm average}$ is usually about 1.5 times larger than $B_{\rm bridge}$, although there is significant scatter about this value.

Thermal pressure around the radio source is estimated using X-ray data as described in § 3.1. It is worth mentioning that for a given X-ray luminosity, the thermal pressures $P_{\rm th} \propto a_c^{-3/2} T^{3/4}$. Thus clusters without measured values of the X-ray temperature T and the X-ray core radius a_c can have large errors on the estimated values of $P_{\rm th}$.

Because of the relatively large errors associated with the thermal and nonthermal pressures estimated as described above, $P_{\rm th}$ and P_{nth} are assumed to be roughly equal if they are within a factor of 3 of each other.

In Figure 6, the thermal pressure of the X-ray emitting gas around FR II sources versus the nonthermal pressure inside the FR II sources is plotted. The solid line in the figure indicates $P_{\rm th} = P_{nth}$, and the dashed lines correspond to where $P_{\rm th}$ is within a factor of 3 of P_{nth}.

It can be seen that most of the points fall into, or point toward the "equilibrium" zone where the thermal and nonthermal pressures are roughly equal.

It is perhaps not surprising to see that the only two cases where P_{nth} is significantly larger than $P_{\rm th}$ are the compact sources 3C 268.3, and 3C 295, both of which have very small linear sizes. The small sizes of these two sources tend to suggest that they are young, so there may not have been enough time for the bridges to expand and reach thermal equilibrium with the surrounding medium. Further, these sources are likely to be interacting with the interstellar medium rather than the ICM. In either case, pressure equilibrium with the ICM is not expected.

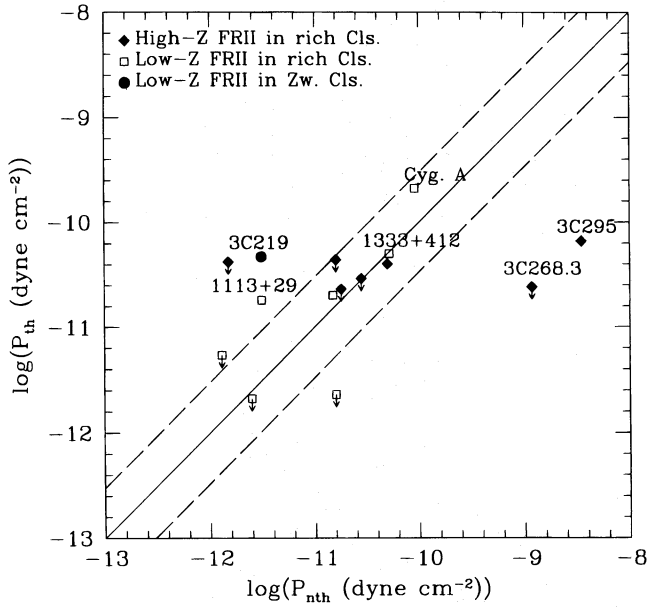

FIG. 6.—The logarithm of the thermal pressures of the ICM around FR II radio galaxies in units of $h^{1/2}$ dyne cm^{-2} vs. the logarithm of the nonthermal pressures in radio bridges of the FR II sources in units of $h^{4/7}$ dyne cm^{-2}. The solid line in the figure shows $P_{\rm th} = P_{nth}$, and the dashed lines correspond to where $P_{\rm th}$ is within a factor of 3 of P_{nth}.

One case where $P_{\rm th}$ is significantly higher than P_{nth} is 3C 219, which is in a Zwicky cluster. In this case, the X-ray emission used to estimate $P_{\rm th}$ is unresolved and is consistent with being pointlike (Miller et al. 1985). Thus, the X-rays could be from the AGN rather than the Zwicky cluster, in which case the thermal pressure estimated using X-ray data is an overestimate.

Another case where $P_{\rm th}$ is higher than P_{nth} is 1113+29, which is in the Abell cluster A1213. This source has also been studied by Morganti et al. (1988). They conclude that the thermal pressure is similar to the nonthermal pressure for this source, contrary to the result obtained here. This discrepancy arises from the different magnetic field strengths obtained. Parma et al. (1986) also give a B field strength for this source that is consistent with the value obtained here. Very few counts were available for the X-ray emission, as noted by Morganti et al. (1988). Thus, in any case, the error in the estimated thermal pressure is large. It is interesting that 1113+29 is an FR II with some FR I characteristics, such as diffuse lobes and weak hot spots. It is quite possible that there might be thermal gas entrained into the radio bridge, which would provide thermal pressure as part of the internal pressure.

Thus, with a few exceptions, there is a trend for the minimum pressures estimated for the radio bridges to be comparable to the thermal pressures of the surrounding gas, although the many limits in the plot make it somewhat difficult to draw a firm conclusion. We proceed under the assumption that nonthermal pressures of the radio bridges of FR II sources are reasonable estimators of ambient gas pressures, although a larger sample with better X-ray and radio maps would be needed to verify this. It is worth mentioning here that there are also other independent observations that tend to indicate pressure equilibrium between radio bridges and their surroundings. For example, the fact that the bridges of many FR II sources do not undergo large amounts of expansion (cf. Wellman & Daly 1996a) and that the B field strength stays roughly constant along these bridges also tend to suggest that rough equilibrium between internal and external pressures has been reached. A direct consequence of this pressure equilibrium is that FR II sources can be used as a diagnostic of their gaseous environments. Such a diagnostic could be very useful where X-ray information is hard to obtain.

4.2.2. *Comparison of Nonthermal Pressure of FR II Sources in Different Environments*

Since the nonthermal pressure of the radio bridge of an FR II source can be a powerful probe of the gaseous environment, a study of P_{nth} values of FR II sources in different galactic environments at different epochs can reveal important information about the gaseous states of these environs.

Figure 7 is a log-linear plot of P_{nth} of the FR II sources versus redshift. Sources with only $B_{\rm average}$ available are circled (see § 4.2.1). When sources with measured values of

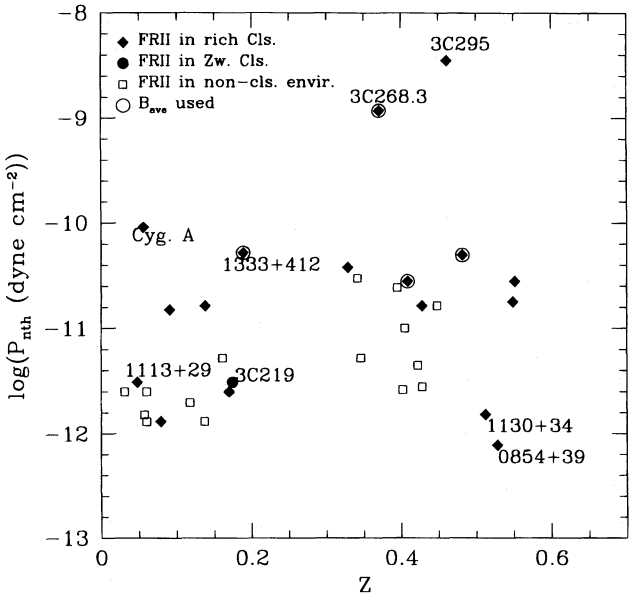

FIG. 7.—The logarithm of the nonthermal pressures in the radio bridges of the FR II sources in units of $h^{4/7}$ dyne cm^{-2} vs. redshift. For sources without detailed bridge information, the average B field strengths are used and are circled in the plot.

the magnetic field across the bridge are considered, it can be seen that most low-redshift FR II radio galaxies have similar P_{nth} values irrespective of whether they are in a rich cluster environment, although there are exceptions, such as Cygnus A. High-redshift FR II's also have P_{nth} values that appear to be independent of whether the source is in a rich cluster environment. Further, the high- and low-redshift FR II radio galaxies have similar P_{nth} values, which becomes more obvious when only sources with B_{bridge} are considered. The two small sources 3C 268.3 and 3C 295 have P_{nth} values that are much higher than other FR II sources. As discussed in §§ 3.2.2 and 4.2.1, these two sources are more likely to be interacting with the ISM and may not have reached pressure equilibria with their environments. Thus, P_{nth} for these sources are not good probes of the ICM around them and should not be compared with other FR II sources.

Since P_{nth} is directly determined by B_{min}, it is also interesting to compare the average B field strengths for FR II sources in different galactic environments. The logarithm of B field strengths of all the FR II sources are plotted in Figure 8 versus their redshifts. As expected, no apparent correlation is seen.

Average and median values of P_{nth} and B_{min} for FR II sources in different galactic environments, both at high and low redshift, are listed in Table 8. The average P_{nth} and B_{min}

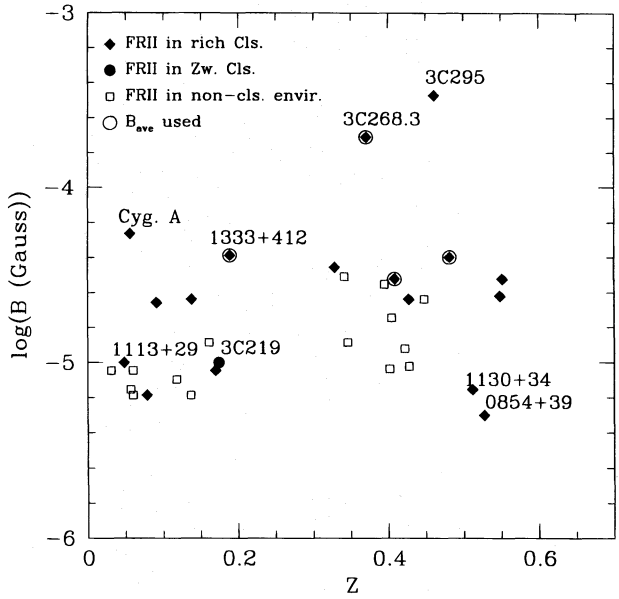

FIG. 8.—The logarithm of the B field strengths in units of $h^{2/7}$ G vs. redshift for FR II sources in different environment. Sources with only $B_{average}$ available are circled in the figure.

TABLE 8

COMPARISON OF P_{nth} AND B_{min}

Radio sources (1)	Subsamples[a] (2)	Number (3)	$\bar{P}_{nth}$[b] (4)	$P_{nth,med}$[b] (5)	$\bar{B}_{min}$[c] (6)	$B_{min,med}$[c] (7)
High-z FR II in clusters[d]	All	7	2.0 ± 0.65	1.8	2.3 ± 0.48	2.4
High-z FR II in clusters[d]	B_{bridge}	5	1.3 ± 0.52	1.6	1.8 ± 0.50	2.3
High-z FR II (non-cluster)[e]	B_{bridge}	6	1.0 ± 0.35	0.73	1.7 ± 0.32	1.5
Low-z FR II in clusters (I)[f]	All	8	2.7 ± 1.1	1.6	2.5 ± 0.61	2.3
Low-z FR II in clusters (I)[f]	B_{bridge}	7	2.4 ± 1.2	1.5	2.3 ± 0.65	2.2
Low-z FR II in clusters (II)[g]	All	7	1.8 ± 0.74	1.5	2.1 ± 0.51	2.2
Low-z FR II in clusters (II)[g]	B_{bridge}	6	1.3 ± 0.57	0.91	1.8 ± 0.45	1.6
Low-z FR II (non-cluster)[e]	B_{bridge}	9	0.57 ± 0.31	0.25	1.1 ± 0.26	0.9
Low-z FR II (Zwicky clusters)[e]	B_{bridge}	1	0.31	...	1.0	...

[a] Two different subsamples are listed according to the type of information available on B field (see § 4.2.1 for details); those denoted "B_{bridge}" include sources with enough information to estimate the bridge magnetic field, and those denoted "All" include sources with and without information on B_{bridge}. For sources without B_{bridge}, the average field strength is used, as described in § 4.2.1.

[b] The average and median (cols. [4] and [5]) nonthermal pressure in units of $10^{-11}\ h^{4/7}$ dyne cm^{-2} (see § 3.1).

[c] The average and median (cols. [6] and [7]) B field strength in units of $10^{-5}\ h^{2/7}$ G (see § 3.1).

[d] Excluding the two compact sources 3C268.3 and 3C295, which most likely are interacting with the interstellar medium (see §4.2.1).

[e] All of the sources have information on B_{bridge}.

[f] Including Cygnus A.

[g] Excluding Cygnus A.

values for low-redshift FR II sources in rich clusters are largely dominated by the P_{nth} and B_{min} of Cygnus A. Thus, we also list the values calculated without Cygnus A.

It can be seen that average values of P_{nth} and B_{min} appear to be similar for all subsamples. At face value, the average P_{nth} and B_{min} for low-redshift FR II sources in noncluster environments are slightly lower than those of FR II sources in other subsamples. However, none of the differences are significant at more than the 1.2 σ level.

Thus, it appears that the FR II sources studied here have similar nonthermal pressures and B field strengths irrespective of their galactic environment and redshift. This suggests that the gaseous environments around these FR II sources have similar thermal pressures as well, provided that equilibrium between the thermal pressure and the nonthermal pressure has been reached.

It is also interesting to note that many of the FR II sources studied here have nonthermal pressures on the order of several times $10^{-12}\ h^{4/7}$ dyne cm^{-2}. In fact, among all the sources whose P_{nth} values are calculated from B_{bridge} instead of $B_{average}$, Cygnus A is the only one that has a P_{nth} value that is similar to typical gas pressures in X-ray bright clusters of galaxies. Typical thermal pressures in the centers of bright X-ray clusters are usually around $5 \times 10^{-11}\ h^{1/2}$ dyne cm^{-2} (cf. PP88 and Jones & Forman 1984). The low nonthermal pressures in the bridges of most FR II sources, combined with the apparent equilibrium between the thermal pressure and the nonthermal pressure seen in the FR II sample, suggest that the systems containing FR II sources, whether optically rich or poor, have gas pressures that are much lower than those of bright X-ray clusters. Such a result is consistent with the scenario that the high pressure of the ICM in a rich cluster prevents FR II sources from forming.

The low pressures in optically rich clusters containing FR II sources could result from low gas temperatures or low gas densities. As a result, such clusters are usually expected to have low X-ray luminosities, as is confirmed by X-ray data in § 5.

4.2.3. *Nonthermal Pressure versus Radio Power*

The fact that the radio power of the FR II sources evolves strongly with redshift while the B field strength and nonthermal pressure do not exhibit strong redshift evolution points to the lack of a strong correlation between radio power and nonthermal pressure. The nonthermal pressure of all the FR II sources are plotted in Figure 9 versus their radio power at 408 MHz. It can be seen that P_{nth} does not appear to be strongly dependent on radio power, as expected; this result is more obvious when only sources with B_{bridge} are considered. For a given radio power, there is a large amount of scatter in B and P_{nth}, and vice versa.

Instead of using the total radio power and the total volume of the source, the bridge B field strengths of the FR II sources studied here are estimated at different points along the radio bridges, using the surface brightness and the bridge width at each point. To estimate the bridge width it is assumed that the bridge is cylindrically symmetric with constant volume emissivity (locally), and the width is obtained by convolving with a Gaussian beam the same size as that used to observe the source, and comparing with the observations. The nonthermal pressure estimated using B_{bridge} is thus determined by bridge conditions, whereas the radio luminosity of an FR II radio source is largely dominated by emission from the radio hot spots. The lack of dependence of bridge nonthermal pressure on radio power points to a large amount of scatter in bridge surface brightness and width for a given radio power. This suggests that the environment is important in determining parameters such as bridge width and brightness, which in turn determine the bridge pressure, but may be less important in determining the radio power of the hot spots.

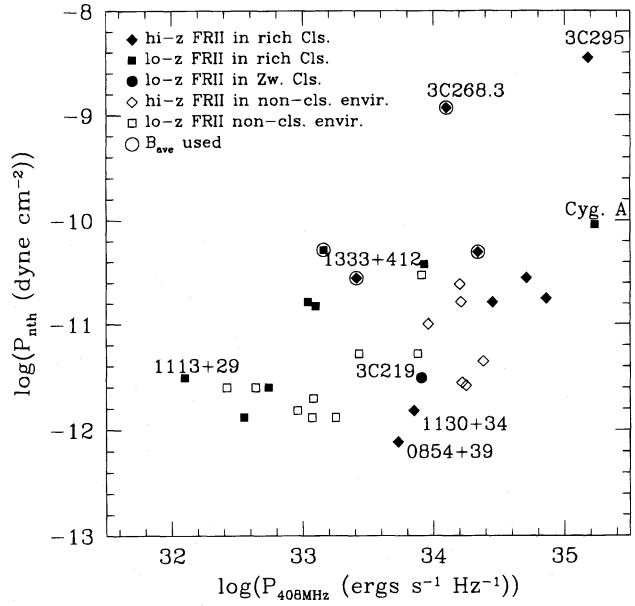

FIG. 9.—The logarithm of the nonthermal pressure in units of $h^{4/7}$ dyne cm^{-2} vs. the logarithm of the total radio power at 408 MHz in units of h^{-2} ergs s^{-1} Hz^{-1} for FR II radio galaxies in different environments. Circled points in the plot are sources with only $B_{average}$ available.

4.3. *Conclusions*

The primary conclusions of the study of FR II radio galaxies in different galactic environments and at different redshifts are as follows.

1. At both low- and high-redshift, FR II sources in rich clusters appear to be similar to FR II sources in noncluster environments at the same epoch in terms of radio power, emission-line and optical properties of the host galaxy, and linear size. High-redshift FR II radio galaxies have higher P_{408} and L_{em} than low-redshift FR II radio galaxies on average, but there are also overlap regions. Magnitudes of host galaxies and linear sizes of FR II sources appear to be similar at high and low redshift.

2. The nonthermal pressures in the radio bridges of many FR II sources are consistent with being in equilibrium with the thermal pressures of the ICM around them, which means that the bridges of many FR II sources in clusters may be thermally confined. This result, if confirmed by a larger sample, would allow FR II sources in clusters to be used as powerful probes of their gaseous environments.

3. In spite of the evolution in radio power and emission-line luminosity with redshift, most high- and low-redshift FR II sources have similar B field strengths and nonthermal pressures irrespective of their galactic environments. Their nonthermal pressures are usually much lower than the typical thermal pressures at the centers of X-ray bright clusters.

4. Together, results 2 and 3 presented above suggest that most FR II sources inhabit systems of relatively low gas

pressure irrespective of redshift. A prediction of this result is that the clusters with FR II sources are expected to have relatively low X-ray luminosities, which is shown to be the case in § 5.

5. RESULTS ON CLUSTERS WITH AND WITHOUT FR II SOURCES

The study in § 4 suggests that many clusters containing FR II sources are expected to have low gas pressures and thus low X-ray luminosities. In this section, X-ray luminosities of clusters with FR II sources are compared with those of clusters without FR II sources to test whether this is the case. The comparison at low-redshift is presented in § 5.1, that at high-redshift is in § 5.2, and in § 5.3 high- and low-redshift clusters without FR II sources are compared. The conclusions of this section are presented in § 5.4.

X-ray luminosities for clusters with and without FR II sources are shown in Figures 10 and 11, where the low-redshift cluster sample included in Figure 10 is that of AK83, while that included in Figure 11 is that of HSB82 (see the discussions in § 2.2). The X-ray luminosities of FR II sources in poor Zwicky clusters and noncluster environments are also plotted for comparison. In addition, the X-ray selected EMSS sources are included in both figures.

Similar conclusions are indicated by both figures. At low redshift, clusters containing FR II radio sources have low X-ray luminosities relative to other clusters. For a high-redshift, it is difficult to draw a firm conclusion due to lack of high-quality data, although the fact that most clusters containing FR II sources only have upper bounds on their X-ray luminosities is consistent with them being underluminous in the X-ray. The fact that similar conclusions are indicated by a comparison with any of the cluster samples without FR II sources suggests that selection effects have not seriously biased the result.

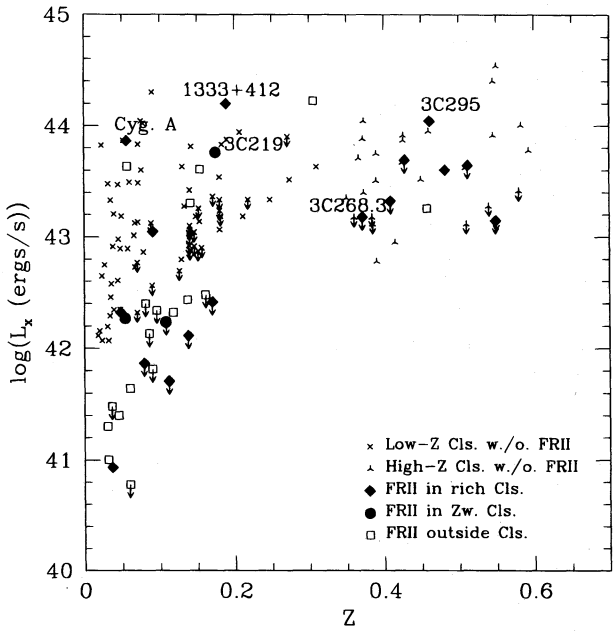

FIG. 10.—The logarithm of the X-ray luminosity in the energy band 0.5–2 keV in units of h^{-2} ergs s^{-1} vs. redshift for clusters with and without FR II sources and for FR II sources in different environments. The X-ray selected EMSS sources are denoted as stars to be differentiated from other optically or radio selected clusters. The low-redshift clusters without FR II sources plotted are those from AK83.

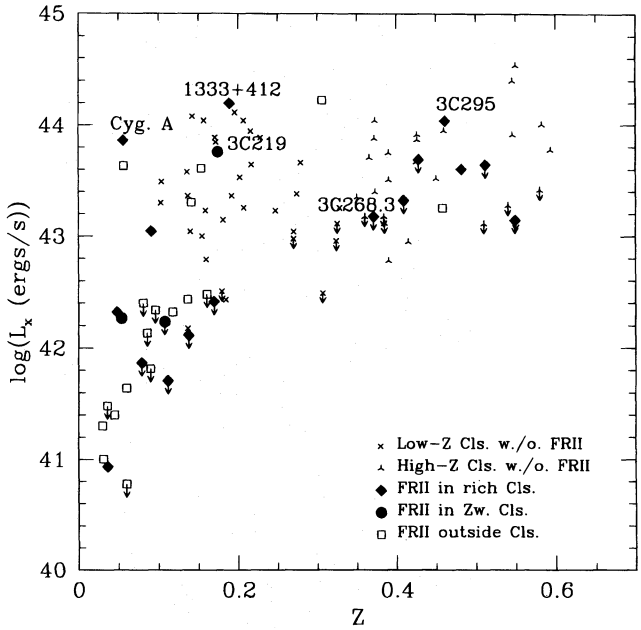

FIG. 11.—The logarithm of the X-ray luminosity in the energy band 0.5–2 keV in units of h^{-2} ergs s^{-1} vs. redshift for clusters with and without FR II sources and for FR II sources in different environments. The low-redshift clusters without FR II sources plotted are those from HSB82.

Average and median X-ray luminosities for clusters with and without FR II sources, both at high and low redshifts, are listed in Table 9 for comparison.

5.1. *Low-Redshift Clusters*

An apparent feature seen in Figures 10 and 11 is that while the X-ray luminosities of low-redshift rich clusters with FR II sources span a large range, most of them are low compared to other rich low-redshift clusters without FR II sources. Except for A1763, in which 1333+412 is the brightest optical member (VB82), 3C 219, and the cluster around Cygnus A, all the low-redshift clusters with FR II sources lie at the lower end of the X-ray luminosity distribution. The cluster A1763 has a relatively large core radius of 270 h^{-1} kpc; thus its high X-ray luminosity is more likely a result of a large X-ray emitting volume rather than a high gas density or pressure. As discussed in § 4.2.1, the X-ray emission from 3C 219 is likely to be due to the AGN rather than the Zwicky cluster around it. Cygnus A appears to be the only low-redshift FR II in a high-pressure gaseous environment, and this is reflected in its high nonthermal pressure.

It is clear from Figures 10 and 11 that some FR II sources in noncluster environments have X-ray luminosities comparable to those of X-ray bright clusters. Thus, AGNs could contribute significantly to the X-ray emission of clusters with FR II sources. Whether the observed X-ray emission is from the AGN or from ambient gas with properties similar to that of gas in poor clusters or groups needs to be determined by X-ray observations with high spatial resolution. However, the discussion in § 3.2.1 suggests that AGN emission might be important. In any case, the low X-ray luminosities are consistent with the low nonthermal pressures found in the radio bridges of these FR II sources (see § 4) and suggests that the gaseous states in X-ray dim clusters with FR II sources are similar to those in noncluster environments.

Average and median X-ray luminosities of low-redshift clusters with FR II sources are listed in Table 9. The

TABLE 9

X-RAY COMPARISON

Clusters (1)	Subsamples (2)	$\bar{L}_X$[a] (3)	$L_{X(median)}$[a] (4)	N_{cls}[b] (5)	N_{bounds}[c] (6)
Low-z Clusters with FR II	All	2.8 ± 1.8	0.21	9	4
Low-z Clusters with FR II	Excluding 1333+42, Cygnus A	0.26 ± 0.14	0.13	7	4
High-z Clusters with FR II.....	Excluding 3C 268.3	4.6 ± 1.4	4.2	6	4
High-z Clusters with FR II.....	Excluding 3C 268.3, 3C 295	3.4 ± 0.7	4.0	5	4
Low-z Clusters without FR II	AK83	2.55 ± 0.39	1.33	72	20
Low-z Clusters without FR II	H82	3.75 ± 0.66	2.0	33	6
High-z Clusters without FR II (I)[d]	All	6.42 ± 1.51	4.0	26	7
High-z Clusters without FR II (I)[d]	Excluding 0016+1609, 0451.6−0305	4.46 ± 0.66	3.3	24	7
High-z Clusters without FR II (II)[e].....	All	5.02 ± 1.71	2.6	17	7
High-z Clusters without FR II (II)[e].....	Excluding 0016+1609	3.46 ± 0.74	2.3	16	7

[a] The average and median (cols. [3] and [4]) X-ray luminosity in the rest frame energy band 0.5–2 keV in units of $10^{43}\ h^{-2}$ ergs s^{-1}.
[b] Total number of clusters in the subsample.
[c] Number of clusters that only have upper bounds on L_X; these bounds were included as detections.
[d] Including EMSS sources.
[e] Excluding EMSS sources.

average luminosities are dominated by the two X-ray bright clusters around Cygnus A and 1333+42. When these two clusters are excluded, the average X-ray luminosities become about an order of magnitude smaller. Thus the median X-ray luminosity is probably a better indicator of the X-ray properties of these clusters as a group.

The median X-ray luminosities of low-redshift clusters with FR II sources are about 5–10 times smaller than those of low-redshift clusters without FR II sources. When Cygnus A and 1333+42 are excluded, the average X-ray luminosity of low-redshift clusters with FR II sources is 10–15 times smaller than those of clusters without FR II sources, which is significant at the 5 σ level.

More recent X-ray observations of low-redshift ($0.03 < z < 0.15$) Abell clusters by Burg et al. (1994) indicate that $L_{X,med} = 0.37 \times 10^{43}\ h^{-2}$ ergs s^{-1} for clusters of Abell class 0 (A0), $L_{X,med} = 0.71 \times 10^{43}\ h^{-2}$ ergs s^{-1} for A1 clusters, and $L_{X,med} = 4.03 \times 10^{43}\ h^{-2}$ ergs s^{-1} for A2 clusters. The clusters with FR II sources studied here have richness classes ranging from A0 to A3, yet have a median X-ray luminosity that is lower than that of A0 clusters. Clearly, these clusters are underluminous in the X-ray.

Thus, while individual FR II sources sometimes appear in rich clusters of galaxies, most tend to lie in clusters with low X-ray luminosities and avoid the most X-ray luminous clusters. This is consistent with the predictions made in § 4 based on the low nonthermal pressures of these FR II sources.

5.2. *High-Redshift Clusters*

At face value, the six high-redshift clusters with FR II sources other than 3C 268.3 appear to cover about the same range of X-ray luminosity as other high-redshift clusters without FR II sources in Figures 10 and 11. However, it is important to keep in mind that 3C 295 is more likely to be interacting with the ISM instead of the ICM, and that four out of the five remaining clusters with FR II sources only have upper bounds on their X-ray luminosity as opposed to detections. Furthermore, there might be a significant AGN contribution to the observed X-ray luminosities of these clusters, as discussed in § 3.2.1.

Average and median X-ray luminosities of the six high-redshift clusters with FR II sources are listed in Table 9; those excluding 3C 295 are also listed. The numbers for the two samples of high-redshift clusters without FR II sources, one with and one without the EMSS sources, are also listed. The average X-ray luminosity for the sample with EMSS sources is dominated by the two very X-ray luminous clusters, 0016+1609 and 0451.3−0305, while that for the sample without the EMSS sources is dominated by 0016+1609. Thus the median X-ray luminosities for the two samples are better indicators of their average X-ray properties; the numbers without those dominant sources are also listed in the table.

The high-redshift sample with EMSS sources have a slightly higher average X-ray luminosity than other high-redshift samples, presumably because the EMSS sources are X-ray selected.

At face value, the high-redshift clusters with FR II sources appear to have an average X-ray luminosity comparable to those of other high-redshift clusters, for both comparison samples used. But the large number of upper bounds on the X-ray luminosities of clusters with FR II sources and a possible AGN contribution to the X-ray emission make this result open to further consideration. One of the results obtained in § 4 is that high-redshift clusters containing FR II sources should be similar to their low-redshift counterparts in terms of thermal pressure of the ICM because the nonthermal pressures of the FR II sources in these clusters are similar to those at low redshift. As a result, the high-redshift clusters with FR II sources are expected to have X-ray luminosities similar to low-redshift clusters with FR II sources. This means that the X-ray luminosities of the ICM of these clusters are predicted to be much lower than the current bounds.

5.3. *High- and Low-Redshift Clusters without FR II Sources*

The X-ray luminosities of high- and low-redshift clusters without FR II sources studied here appear to cover about the same range in Figures 10 and 11. For the high-redshift sample without EMSS sources, the mean X-ray luminosity is slightly higher than that of the low-redshift clusters. This is largely due to one very X-ray luminous cluster: 0016+1609. When this cluster is excluded, the high-redshift clusters without FR II sources appear to have an average X-ray luminosity comparable to that of the low-redshift

clusters. Average and median X-ray luminosities for the high-redshift sample including EMSS sources are slightly higher than those without EMSS sources and are also slightly higher than those of low-redshift clusters without FR II sources. This is probably because high-redshift clusters with very low X-ray luminosities are missing in a flux-limited sample such as EMSS.

5.4. *Conclusions*

1. X-ray luminosities of low-redshift clusters with FR II sources tend to lie at the lower end of cluster X-ray luminosity distribution. On average, these clusters appear to be underluminous in the X-ray compared with low-redshift clusters without FR II sources. This is in agreement with predictions made in § 4 about the X-ray luminosities of these clusters based on the nonthermal pressures of their radio bridges.

2. The high-redshift X-ray data are inconclusive because most of the clusters with FR II sources have only upper bounds on their X-ray luminosities as opposed to detections. Also, AGN contributions to the observed X-ray luminosities may be significant. Based on results from § 4 that most high-redshift FR II radio galaxies in clusters have nonthermal pressures as low as their low-redshift counterparts, many of the high-redshift clusters with FR II sources are expected to have low X-ray luminosities, luminosities similar to those of their low-redshift counterparts. Thus the X-ray luminosities of the ICM of these clusters are predicted to be well below the current bounds.

3. High- and low-redshift clusters without FR II sources studied here appear to be similar to each other in terms of X-ray luminosity.

6. SUMMARY AND DISCUSSION

The purpose of this study was to establish whether the lack of FR II sources in rich clusters of galaxies at low redshift is related to the presence of the hot intracluster medium (ICM), and whether the presence of FR II sources in high-redshift clusters is related to an evolution of the ICM. The key diagnostics are the nonthermal pressure of the radio bridge and the X-ray luminosity and gas pressure of the ICM. By using the low-redshift data it was established that the nonthermal pressure of the radio bridge, estimated using the minimum energy magnetic field, is typically within a factor of 3 of the ambient gas pressure, estimated using the X-ray luminosity of the ICM. Thus, in most cases, the nonthermal pressure of the radio bridge may be used as a rough estimate of the pressure of the ICM; the exceptions to this rule are understood and are discussed in § 4.2.1.

Two key results emerged from this study. The first is that the nonthermal pressures of the radio bridges of the FR II radio galaxies studied seem to be independent of environment and redshift. This suggests that these FR II sources are in regions with similar gas pressure. Thus, although the radio power of the sources studied tends to increase systematically with redshift, the bridge pressures of the sources do not appear to shift with redshift.

The second key result is that the X-ray luminosities of low-redshift clusters with FR II sources generally lie at the low end of the X-ray distribution of optically similar clusters without FR II sources and often have X-ray luminosities comparable to those of FR II sources in noncluster environments. This conclusion can only be established at low redshift, where the cluster X-ray emission is generally a detection rather than a bound and is often resolved and can be attributed to ICM rather than AGN emission.

The combination of the two key results suggests that rich clusters at redshifts of about 0.5 with FR II sources have an ICM with low gas pressure compared with optically similar low-redshift clusters. This leads to the prediction that ICM X-ray emission from these clusters will have a low X-ray luminosity, comparable to low-redshift clusters with FR II sources. This cannot be checked observationally at present due to the large number of upper bounds on the X-ray luminosities and the fact that detected emission is generally unresolved and could originate from either the ICM or the AGN.

The observations suggest that the evolution of the environments of FR II sources with redshift is related to an evolution of the ICM in the sense that the pressure of the ICM decreases with increasing redshift. The negative evolution of the pressure of the ICM of rich clusters of galaxies with redshift suggested here is consistent with the negative evolution of the cluster X-ray luminosity function (Gioia et al. 1990; Edge et al. 1990; H92; Castander et al. 1994; Bower et al. 1994), the lack of evolution of optical clusters with redshift (cf. Gunn, Hoessel, & Oke 1986), the fact that optically rich clusters at a redshift of about 0.5 have lower X-ray luminosities than optically similar low-redshift clusters (Bower et al. 1994), and the negative evolution of the ambient gas density in the vicinity of very powerful radio sources with redshift seen out to much larger redshifts (Daly 1995; Wellman & Daly 1996b, 1996c). However, it is interesting to note that despite the negative evolution of the cluster X-ray luminosity function, there are X-ray luminous clusters detected at high redshift (cf. Luppino & Gioia 1995). Luppino & Gioia (1995) show that the X-ray luminosity function constructed using the high-redshift clusters they observed and the clusters observed by Castander et al. (1994) is consistent with the luminosity function constructed using the EMSS clusters (H92), which exhibits negative redshift evolution.

A few different physical pictures can account for the evolution of the ICM indicated here and by other studies. For example, the ICM in some of the high-redshift, optically rich clusters may not be in place yet, and thus these clusters are capable of supporting FR II sources. This could occur if a large portion of the gas is still in individual galaxies at early epochs rather than in the intracluster medium. Later, dynamical evolution could release the gas into the ICM via galaxy-galaxy collisions, ram pressure stripping, tidal stripping, etc., and thus create a hot, dense ICM that suppresses FR II sources from appearing. Another picture is one in which the gaseous cores of the clusters are slowly cooling and condensing, which would increase the core gas density and lead to higher pressure gaseous cores.

A different model to explain the different environments of FR I and II sources and their evolution has been proposed by Baum, Zirbel, & O'Dea (1995). They suggest that FR II sources are associated with central black holes with high accretion and spin rates, which are likely to be products of merger events. In this model, FR II sources tend to avoid rich environments because the higher velocity dispersions in such environments tend to suppress merger activity. The evolution of the environments of FR II sources can then be explained if there are more merger events in clusters at high-redshift. This model may be consistent with the results

presented here if a higher merger rate is somehow linked to a system having a low gas pressure. The work of Ledlow & Owen (1995), however, suggests that merger events do not play a major role in FR I radio sources.

It is a pleasure to thank Lauren Jones for her work during the early stages of the project, and Roger Blandford, Alan Bridle, Ed Groth, Eddie Guerra, Dan Harris, Simon Lilly, Rick Perley, and Greg Wellman for helpful discussions. This work was supported in part by the National Aeronautics and Space Administration, the US National Science Foundation, and the Independent College Fund of New Jersey.

REFERENCES

Abramopoulos, F., & Ku, W. H.-M. 1983, ApJ, 271, 446
Akujor, C. E., Lüdke, E., Browne, I. W. A., Leahy, J. P., Garrington, S. T., Jackson, N, & Thomasson, P. 1994, A&AS, 105, 247
Akujor, C. E., Spencer, R. E., & Wilkinson, P. N. 1990, MNRAS, 24, 362
Allington-Smith, J. R. 1982, MNRAS, 199, 611
Allington-Smith, J. R., Ellis, R. S., Zirbel, E. L., & Oemler, A., Jr. 1993, ApJ, 404, 521 (AS93)
Arnaud, K. A., Fabian, A. C., Eales, S. A., Jones, C., & Forman, W. 1984, MNRAS, 211, 981
Baum, S. A., Zirbel, E. L., & O'Dea, C. P. 1995, ApJ, 451, 88
Bondi, M., Gregorini, L., Padrielli, L., & Parma, P. 1993, A&AS, 101
Bower, R. G., Bohringer, H., Briel, U. G., Ellis, R. S., Castander, F. J., & Couch, W. J. 1994, MNRAS, 268, 345
Burg, R., Giacconi, R., Forman, W., & Jones, C. 1994, ApJ, 422, 37
Burns, J. O., Basart, J. P., De Young, D. S., & Ghiglia, D. C. 1984, ApJ, 283, 515
Burns J. O., & Gregory, S. A. 1982, AJ, 87, 1245
Burns, J. O., Gregory, S. A., & Holman, G. D. 1981, ApJ, 250, 450
Burns, J. O., Owen, F. N., & Rudnick, L. 1978, AJ, 83, 312
Burns, J. O., Rhee, G., Owen, F. N., & Pinkney, J. 1994, ApJ, 423, 94 (BROP94)
Carilli, C. L., Perley, R. A., Dreher, J. W., & Leahy, J. P. 1991, ApJ, 383, 554
Carilli, C. L., Perley, R. A., & Harris, D. E. 1994, MNRAS, 270, 173
Castander, F. J., Ellis, R. S., Frenk, C. S., Dressler, A., & Gunn, J. E. 1994, ApJ, 424, L79
Clarke, D. A., Bridle, A. H., Burns, J. O., Perley, R. A., & Norman, M. L. 1992, ApJ, 385, 173
Daly, R. A. 1995, ApJ, 454, 580
Eales, S. A. 1985, MNRAS, 217, 149
Edge, A. C., Stewart, G. C., Fabian, A. C., & Arnaud, K. A. 1990, MNRAS, 245, 559
Fabbiano, G., Doxsey, R. E., Johnson, M., Schwartz, D. A., & Schwartz, J. 1979, ApJ, 230, L67
Fabbiano, G., Miller, L., Trinchieri, G., Longair, M., & Elvis, M. 1984, ApJ, 277, 115
Fanaroff, B. L., & Riley, J. M. 1974, MNRAS, 167, 31
Feigelson, E. D., & Berg, C. J. 1983, ApJ, 269, 400 (FB83)
Fernini, I., Burns, J. O., Bridle, A. H., & Perley, R. A. 1993, AJ, 105 (5), 1690
Gioia, I. M., Henry, J. P., Maccacaro, T., Morris, S. L., Stocke, J. T., & Wolter, A. 1990, ApJ, 356, L35
Gioia, I. M., & Luppino, G. A. 1994, ApJS, 94, 583
Gregorini, L., Padrielli, L., Parma, P., & Gilmore, G. 1988, A&AS, 74, 107
Gunn, J. E., Hoessel, J. G., & Oke, J. B. 1986, ApJ, 306, 30
Henry, J. P., Gioia, I. M., Maccacaro, T., Morris, S. L., Stocke, J. T., & Wolter, A. 1992, ApJ, 386, 408 (H92)
Henry, J. P., Soltan, A., & Briel, U. 1982, ApJ, 262, 1 (HSB82)
Hill, G. J., & Lilly, S. J. 1991, ApJ, 367, 1 (HL91)
Jenkins, C. J., Pooley, G. G., & Riley, J. M. 1977, MemRAS, 84, 61
Jones, C., & Forman, W. 1984, ApJ, 276, 38
Laing, R. A. 1981, MNRAS, 195, 261
Laing, R. A., Riley, J. M., & Longair, M. S. 1983, MNRAS, 204, 151
Law-Green, J. D. B., Leahy, J. P., Alexander, P., Allington-Smith, J. R., van Breugel, W. J. M., Eales, S. A., Rawlings, S. G., & Spinrad, H. 1995, MNRAS, 274, 939
Leahy, J. P., Muxlow, T. W. B., & Stephens, P. W. 1989, MNRAS, 239, 401
Leahy, J. P., & Perley, R. A. 1991, AJ, 102, 537
Leahy, J. P., & Williams, A. G. 1984, MNRAS, 210, 929
Ledlow, M. J., & Owen, F. N. 1995, AJ, 110, 1959
Longair, M. S., & Seldner, M. 1979, MNRAS, 189, 433
Luppino, G. A., & Gioia, I. M. 1995, ApJ, 445, L77
Miley, G. K. 1980, ARA&A, 18, 165
Miller, L. 1985, MNRAS, 215, 773
Miller, L., Longair, M. S., Fabbiano, G., Trinchieri, G., & Elvis, M. 1985, MNRAS, 215, 799
Morganti, R., Fanti, R., Gioia, I. M., Harris, D. E., Parma, P., & De Ruiter, H. 1988, A&A, 189, 11
Nilson, K., Valtonen, M. J., Kotilainen, J., & Jaakkola, T. 1993, ApJ, 413, 453
Owen, F. N. 1975, AJ, 80, 263
———. 1976, AJ, 81, 571
———. 1993, in Jets in Extragalactic Radio Sources, ed. H.-J. Röser & K. Meisenheimer (Berlin: Springer), 273
Pacholczyk, A. G. 1970, Radio Astrophysics (San Francisco: Freeman)
Parma, P., Cameron, R. A., & De Ruiter, H. R. 1991, AJ, 102(6), 1960
Parma, P., De Ruiter, H. R., Fanti, C., & Fanti, R. 1986, A&AS, 64, 135
Parma, P., Fanti, C., Fanti, R., Morganti, R., & De Ruiter, H. R. 1987, A&A, 181, 244
Peacock, J. A., & Wall, J. V. 1981, MNRAS, 194, 331
Perley, R. A., Bridle, A. H., Willis, A. G., & Fomalont, E. B. 1980, AJ, 85, 499
Pooley, G. G., & Henbest, S. N. 1974, MNRAS, 169, 477
Prestage, R. M., & Peacock, J. A. 1988, MNRAS, 230, 131 (PP88)
———. 1989, MNRAS, 236, 959
Riley, J. M. 1975, MNRAS, 170, 53
Rudnick, L., & Owen, F. N. 1977, 82 (1), 1
Signal, A. K. 1993, MNRAS, 263, 139
Sokoloski, J. L., Daly, R. A., & Lilly, S. J. 1994, in AIP Conf. Proc., 313, The Soft X-ray Cosmos, ed. E. M. Schlegel & R. Petre (New York: AIP), 386
———. 1996, ApJ, 459, 142
Vallée, J. P., & Bridle, A. H. 1982, ApJ, 253, 479 (VB82)
van Breugel, W., Miley, G., & Heckman, T. 1984, AJ, 89 (1), 5
Wall, J. V., & Peacock, J. A. 1985, MNRAS, 216, 173
Wellman, G. F., & Daly, R. A. 1996a, in Cygnus A—Study of a Radio Galaxy, ed. C. L. Carilli & D. E. Harris (Cambridge: Cambridge Univ. Press), in press
———. 1996b, in Cygnus A—Study of a Radio Galaxy, ed. C. L. Carilli & D. E. Harris (Cambridge: Cambridge Univ. Press), in press
———. 1996c, in preparation
Yates, M. G., Miller, L., & Peacock, J. A. 1989, MNRAS, 240, 129 (YMP89)
Yee, H. K. C., & Green, R. F. 1984, ApJ, 280, 79
———. 1987, ApJ, 319, 28
Zirbel, E. L., & Baum, S. A. 1995, ApJ, 448, 548 (ZB95)